

Simulating the effects of quasar structure on parameters from geodetic VLBI

Stanislav S. Shabala¹ · Jamie N. McCallum¹ · Lucia Plank¹ · Johannes Böhm²

Received: 6 September 2013 / Accepted: 17 April 2015 / Published online: 13 May 2015
© Springer-Verlag Berlin Heidelberg 2015

Abstract We investigate the effects of quasar structure on geodetic very long baseline interferometry (VLBI) measurements. We create catalogues of simulated and real quasars with a range of structure indices, and use these to generate synthetic CONT11 observations with the Vienna VLBI Software simulator tool. We systematically investigate the effects of quasars with different amounts of source structure, and find that source structure can affect station positions at the one-millimetre level. This effect is stronger for isolated stations. Overall, source structure is found to contribute to about 10 % of the troposphere and clock effects. Our simulations confirm analytical predictions that source structure mitigation strategies must be developed in order to achieve millimetre-level VLBI position accuracy.

Keywords Geodesy · Very long baseline interferometry (VLBI) · Astrometry · Celestial reference frame (CRF)

1 Introduction and motivation

In recent years, many investigations and simulations have been carried out to identify the best possible observing strategies and antennas for the next generation geodetic VLBI system, VLBI2010, now also referred to as VLBI global observing system (VGOS), with the ambitious goals of 1 and 0.1 mm/year accuracy in station position and velocity, respectively (Plag and Pearlman 2009). A series of Monte Carlo simulations carried out by the VLBI groups at Goddard Space Flight Center and the Vienna University of Technology led to the conclusion that the troposphere is the dominating error source, and that smaller and faster antennas should be used to increase the number of observations, thus mitigating tropospheric effects; it was also recommended that broadband receiving systems from 2 to 14 GHz should be applied (Petrachenko et al. 2009). All those simulations accounted for tropospheric turbulence, clock errors, and instrumental errors (see e.g. Pany et al. 2011); however, the effects of source structure have not been considered so far. Here, we assess the influence of source structure on station positions and Earth rotation parameters (ERPs) as derived from the schedules used in the CONT11 VLBI campaign. In Sect. 2, we introduce the formalism behind our source structure simulations. We describe our catalogues of source structure in Sect. 3, and present results in Sect. 4. We conclude in Sect. 5.

2 Visibilities and structure indices

Radio-loud quasars making up the International celestial reference frame (ICRF2; Ma et al. 2009) are not point sources. They often have structure, with VLBI imaging showing jets in addition to compact cores. This structure also evolves signifi-

✉ Stanislav S. Shabala
Stanislav.Shabala@utas.edu.au

Jamie N. McCallum
Jamie.McCallum@utas.edu.au

Lucia Plank
Lucia.Plank@utas.edu.au

Johannes Böhm
johannes.boehm@tuwien.ac.at

¹ School of Physical Sciences, University of Tasmania, Private Bag 37, Hobart, TAS 7001, Australia

² Department of Geodesy and Geoinformation, Vienna University of Technology, Gusshausstrasse 27-29, 1040 Vienna, Austria

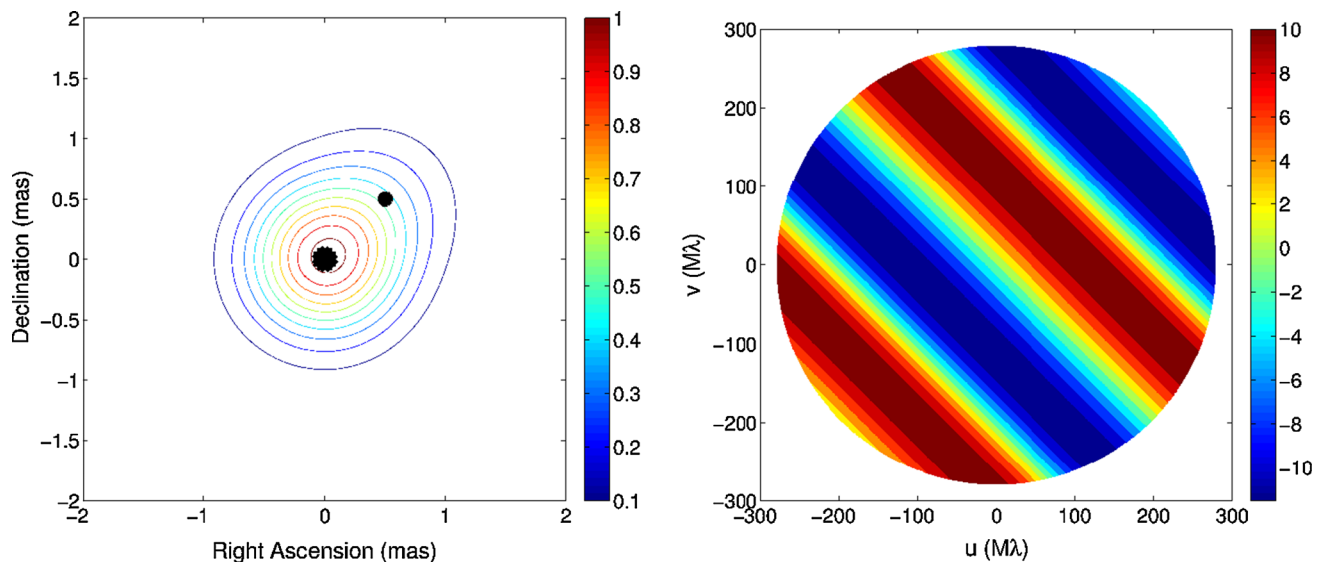


Fig. 1 *Left panel* simulated two-component source with structure index 2.7. The flux density ratio of the two components (*filled circles*) is 5:1. Each component is modelled as a δ -function, and the structure is convolved with a 1 mas beam. *Colours* represent scaled flux density.

Right panel visibility phase. Structure phase is constant in the direction orthogonal to the vector joining the two source components. *Colours* represent structure phase in degrees

cantly over time (e.g. Lister et al. 2009), with jet components appearing and disappearing.

In a seminal paper, Charlot (1990) developed the formalism for estimating the effects of source structure on geodetic VLBI group delays. He showed that for a non-point source, there will be a non-zero contribution to the group delay from source structure as observed phase varies with frequency.

The observed phase depends on projected structure as seen by a given baseline. This, in turn, is a function of baseline length, the relative orientation of the jet axis and observing baseline (which changes as the Earth rotates), and source component separation and brightness ratios. The various components making up the radio source structure will beat in and out of phase, and this effect is slightly different at each of the eight X-band sub-bands, due to the different observing frequencies. Therefore, source structure contributes different phase terms in each sub-band, and therefore the group delay (which is just the slope of phase across frequency sub-bands) also changes.

It is convenient to define the complex visibility function as a Fourier Transform of the source brightness distribution. This visibility function is represented in the UV plane, which is essentially the North–East plane projected in the source direction. Distances in the UV plane are measured in units of observing wavelength, and so the same physical point will have a different location in the UV plane as the observing frequency changes. The visibilities measured by an interferometer represent amplitudes and phases sampled at discrete locations in the UV plane (e.g. Charlot 1990).

We illustrate this process in Fig. 1. The left panel shows a simulated two-component source, smoothed with a circular Gaussian restoring beam with Full Width at Half Maximum (FWHM) = 1 mas (this value is similar to the size of the synthesised beam on a Hobart–HartRAO baseline at X-band). Visibility phase is shown in the right panel. The direction of phase variations is parallel to the line joining two components. In other words, there is no source structure contribution to the phase in the direction perpendicular to source extension. In Fig. 2, we show the structure delays corresponding to observations of this source at X-band. The left panel shows the structure delay for this source observed with a 9280-km projected baseline oriented parallel to the source extension. This baseline length corresponds to 246–268 million wavelengths ($M\lambda$) in Fig. 1. The slope of phase against frequency yields the group delay due to source structure, $\tau_{\text{str}} = \left(\frac{1}{2\pi}\right) \frac{d\phi}{d\nu}$. The right panel generalises this calculation for a range of projected baselines.

3 Mock catalogues

We used the above formalism to generate two-component mock source structure catalogues as follows.

We simulated a range of two-component sources. There are two important parameters describing such sources (e.g. Charlot 1990): the brightness ratio of the two components, and their separation. We assumed each component was a point source; relaxing this assumption in some test cases did not affect the derived structure delays.

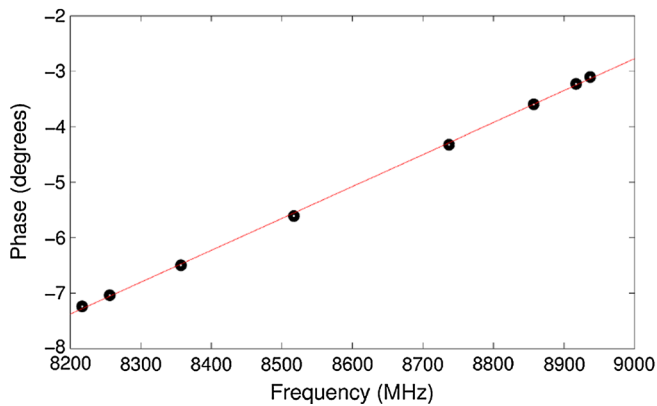
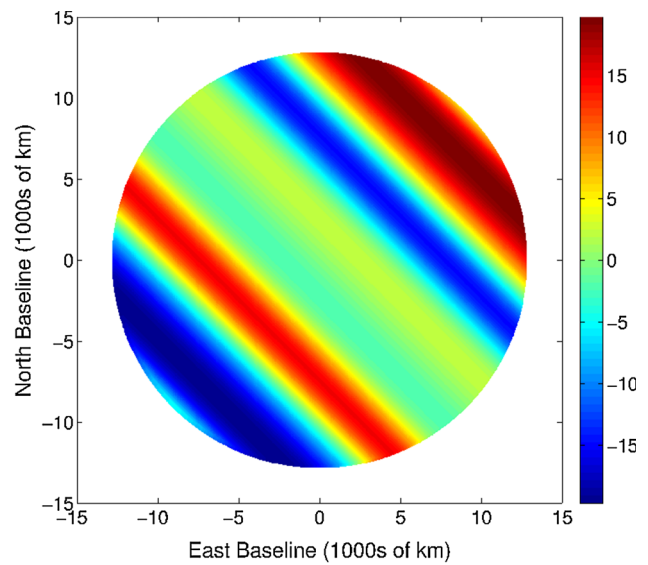


Fig. 2 *Left panel* structure phase as a function of frequency for the source in Fig. 1 observed with a 9280-km baseline parallel to the source jet axis. The structure contribution to the group delay is given by

The brightness ratio was allowed to vary from 0.04 to 0.44. Component separation varied from 0–35 mas, although as we explain below, most of our mock sources have component separations $\lesssim 5$ mas. These values are consistent with VLBI imaging of flat-spectrum quasars (Lister et al. 2009). For each combination of brightness ratio and separation, we calculated the additional phase term due to source structure, for every Earth-bound baseline in a 512×512 grid in the UV plane cf (Fey and Charlot 1997). Repeating this for each of the eight X-band sub-bands, we fitted a slope to the resultant “structure phase” (Fig. 2); this slope yields the group delay as outlined above. We found the median group delay for each source over all Earth-bound baselines, and converted this to structure index (Ma et al. 2009), $SI = 1 + 2 \log(1 + \tau_{str,median}/ps)$.

Of course this mapping between brightness ratio and separation, and source structure index, is not bijective. There are many combinations of brightness ratio and component separation that yield the same structure index. Therefore, when generating mock catalogues (i.e. source models given a structure index), we chose at random the component brightness ratio; this in turn fixed component separation. In our mock ICRF2 catalogue (see below), 15 % of the sources had separations in excess of 5 mas, and less than 1 % in excess of 10 mas; this is consistent with typical observed separations (Lister et al. 2009). The direction of the separation vector (analogous to, e.g. direction of the radio jet in real sources) was assigned at random.

Proceeding in this way, we generated five catalogues. The first four catalogues consist of source models constructed in such a way that each source has a fixed structure index value. We chose these structure indices to be 1, 2, 3 or 4. These



the slope of phase against frequency. *Black points* represent the eight X-band channels. *Right panel* Delay (in picoseconds) due to structure for the source in Fig. 1, as a function of observing projected baseline

catalogues allow us to quantify the effects of different levels of source structure on geodetic VLBI data products.

Real sources of course show different levels of source structure. Our fifth catalogue draws on the observed distribution of structure indices in ICRF2¹. We use this distribution to assign structure indices to individual sources in our mock catalogue, and then follow the procedure above to generate two-component source models.

Ideally, we would like to use real quasar images in our simulations; however, many ICRF2 sources have been imaged rarely (if at all). In addition, quasar structure is variable on timescales of months (Lister et al. 2009; Shabala et al. 2014), and thus only images contemporaneous to the epoch of geodetic observations should be used. Because of this, we use mock catalogues in the present work. However, we test our findings with a final, sixth source structure catalogue, which uses available real source structure images from the Astro-Geo database². As explained below, in this work we choose to simulate CONT11 observations. Imaging data obtained within 2 years of September 2011 were available for 92 of 112 sources observed in CONT11, corresponding to 87 % of the available observations. We did not assign any structure to the remaining 20 quasars, effectively treating them as perfect point sources. Therefore, in the analysis below the simulations using this “real” structure catalogue should

¹ Structure indices for over 700 sources have been observed and tabulated in the Bordeaux VLBI image database (BVID). Many of these have multi-epoch images.

² <http://www.astrogeo.org>.

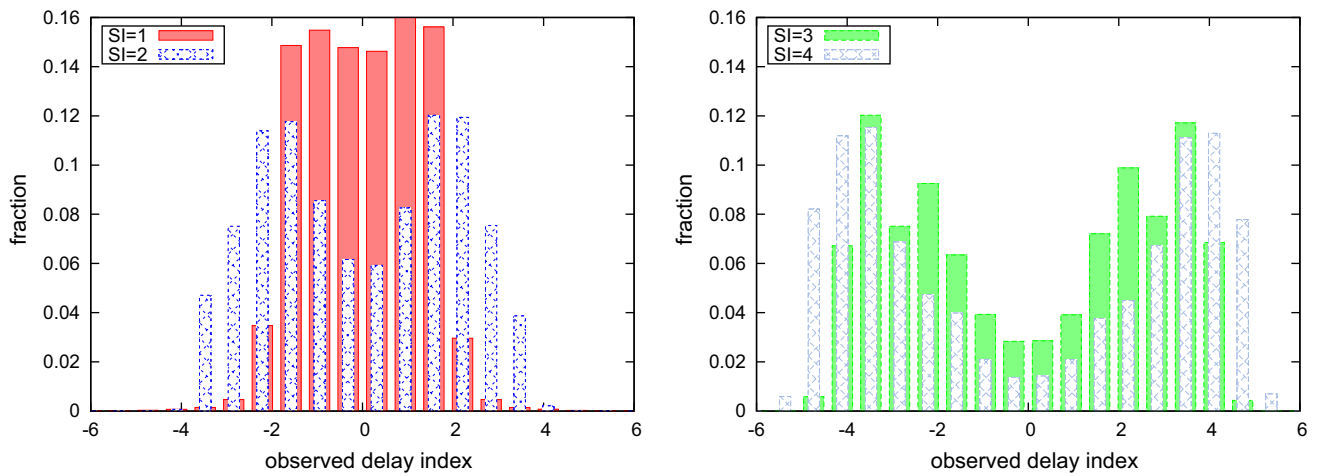


Fig. 3 Distributions of observed delay indices, defined for each source as $1 + 2 \log(\tau_{\text{delay,observed,median}}/\text{ps})$. Although the structure indices (which are based on averaging over all Earth-bound baselines) for each

source are the same (1 and 2 for the *left panel*; 3 and 4 for the *right panel*), the observed delay indices show a wider distribution

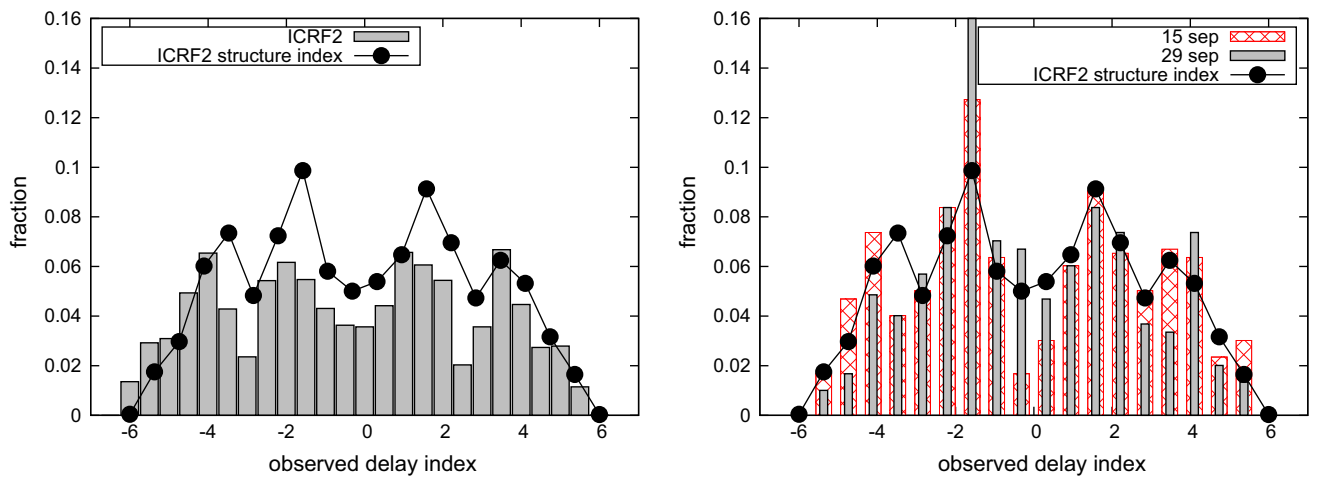


Fig. 4 Distributions of observed delay indices for an ICRF2-like catalogue. *Left panel* distribution for all scans over 15 days of the CONT11 campaign. *Right panel* distributions for two individual sessions. Scheduling plays an important role in determining the observed

delay indices. *Solid line* shows the distribution of structure indices for real ICRF2 sources. For these real sources, we modify the distribution of structure indices to be symmetric about zero, since positive and negative contributions to the group delay are equally likely

be interpreted as providing lower (but realistic) limits to the actual effects of source structure.

It is important to note that the structure index of a source is a quantity defined over all Earth-bound baselines. The actual source structure contribution to the group delay observed on any given baseline will depend on the relative orientations of source structure and the baseline vector. Thus, the observed delay index (derived only from the observed baselines) for each source can be quite different from the expected structure index (as calculated from all possible Earth-bound baselines). We illustrate this point in Figs. 3 and 4, which show the observed distributions of delay indices in our catalogues as observed with the CONT11 schedules. While the peaks in

the distribution are indeed close to the input structure indices (e.g. ± 1 or 2 for the left panel of Fig. 3), there are some significant departures from these values³. This is purely due to network geometry and scheduling.

Histograms in the right panel of Fig. 4 show how different the observed delay index distributions are for the first (15 September) and last (29 September) days of CONT11. We note that these plots represent an integrated quantity (over all scans and baselines), and differences for individual baselines

³ We define observed delay indices to be positive if presence of source structure increases the measured group delay, and negative if the group delay is decreased.

will be even more pronounced. Clearly, scheduling plays an important role in determining exactly what source structure is seen.

4 Source structure simulations

We choose to simulate observations performed during the CONT11 campaign. The CONT campaigns have a number of advantages over regular R1/R4 experiments (Schuh and Behrend 2012). A fixed, large (13 stations⁴) network minimises the effect of network geometry on solutions. The large number of scans (typically at least twice the R1/R4 value) also reduces the uncertainty of the parameters. Furthermore, 15 days of continuous observing with (almost) the same network but different schedules (i.e. different projected quasar structure even on the same baselines) provide the ideal test bed to evaluate the effects of source structure on geodetic measurements.

We present two types of simulations with the Vienna VLBI Software (VieVS, Böhm et al. 2012): (1) source structure only; and (2) source structure plus tropospheric turbulence and clock errors.

4.1 Structure-only simulations

In the first instance, we use the catalogues described in Sect. 3 to simulate the effects of source structure. We simulate each day of CONT11 30 times using seven different catalogues. The first catalogue contains no source structure, i.e. the quasars are assumed to be perfect point sources. Four sets of simulations use catalogues with structure indices of 1, 2, 3 and 4, corresponding to median group delay due to source structure of 1, 3, 10 and 30 ps, respectively. The fifth simulation uses our mock ICRF2 catalogue, where individual quasars have different structure indices, but the distribution of structure indices for all simulated ICRF2 quasars is equivalent to that measured for the real ICRF2 sources (see Ma et al. 2009). Significant effort has recently gone into careful selection of sources for geodetic VLBI observations, and frequently observed sources typically show lower structure indices than those drawn at random from the ICRF2 catalogue. Because of this, we construct a final catalogue containing real images of sources observed during the CONT11 campaign. The distribution of structure indices for these real sources is shown in Fig. 5. Of the 112 observed sources, 20 sources (corresponding to 13 % of the observations) did not have available images within a 2-year window of September 2011. For the purposes of this work, we conservatively

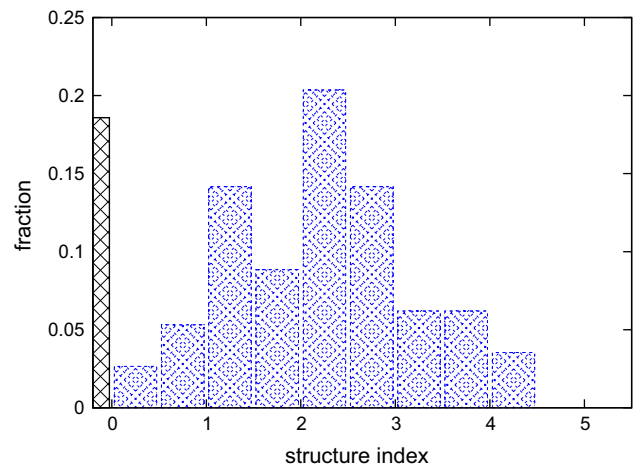


Fig. 5 Distribution of structure indices for sources observed during the CONT11 campaign. *Blue histogram* shows the source structure index in September 2011. Sources with no available structure index information are shown as a *black-and-white shaded histogram* near SI = 0

assumed that these do not have any structure; our results for the effects of “real” source structure of geodetic VLBI observables are therefore, strictly speaking, lower limits.

In all simulations, we use real sky positions and projected baseline scans for all sources, but in the case of mock catalogues replace actual source structure with our simulated catalogues. We note that we do not attempt to reproduce CONT11 observations with our simulations. Instead, we use CONT11 schedules to assess the impact of different levels of source structure on geodetic solutions. We also ran an additional simulation using the “real” source structure catalogue, and compared the results to our mock catalogues.

To each group delay, we add 1 ps rms of white noise. We note that while we model instrumental noise (and later also the troposphere and clocks) as random errors, source structure effects are simulated as systematic errors that depend on the observing strategy. For weighting the observations in all sessions, we used the original delay uncertainties as provided in the (observed) CONT11 NGS files, and added 1 cm uncertainty in quadrature.

We estimate daily station coordinates applying an NNR/NNT condition on all CONT11 stations. Furthermore, we estimate daily Earth orientation parameters (polar motion, UT1-UTC, celestial pole offsets). As auxiliary parameters we estimate zenith wet delays as piecewise linear offsets every 60 min with a relative constraint of 1.5 cm after 60 min; tropospheric north and east gradients as piecewise linear offsets every 6 h with relative constraints of 0.5 mm after 6 h; and quadratic clock polynomials and piecewise linear offsets for the clocks every 60 min with relative constraints of 1.3 cm after 60 min. Source coordinates were fixed.

Below we compare our solutions using station positions and Earth orientation parameters.

⁴ A 14th station, Warkworth (New Zealand), participated in the September 26 session. Because this station was only included in one session, we exclude it from our analysis.

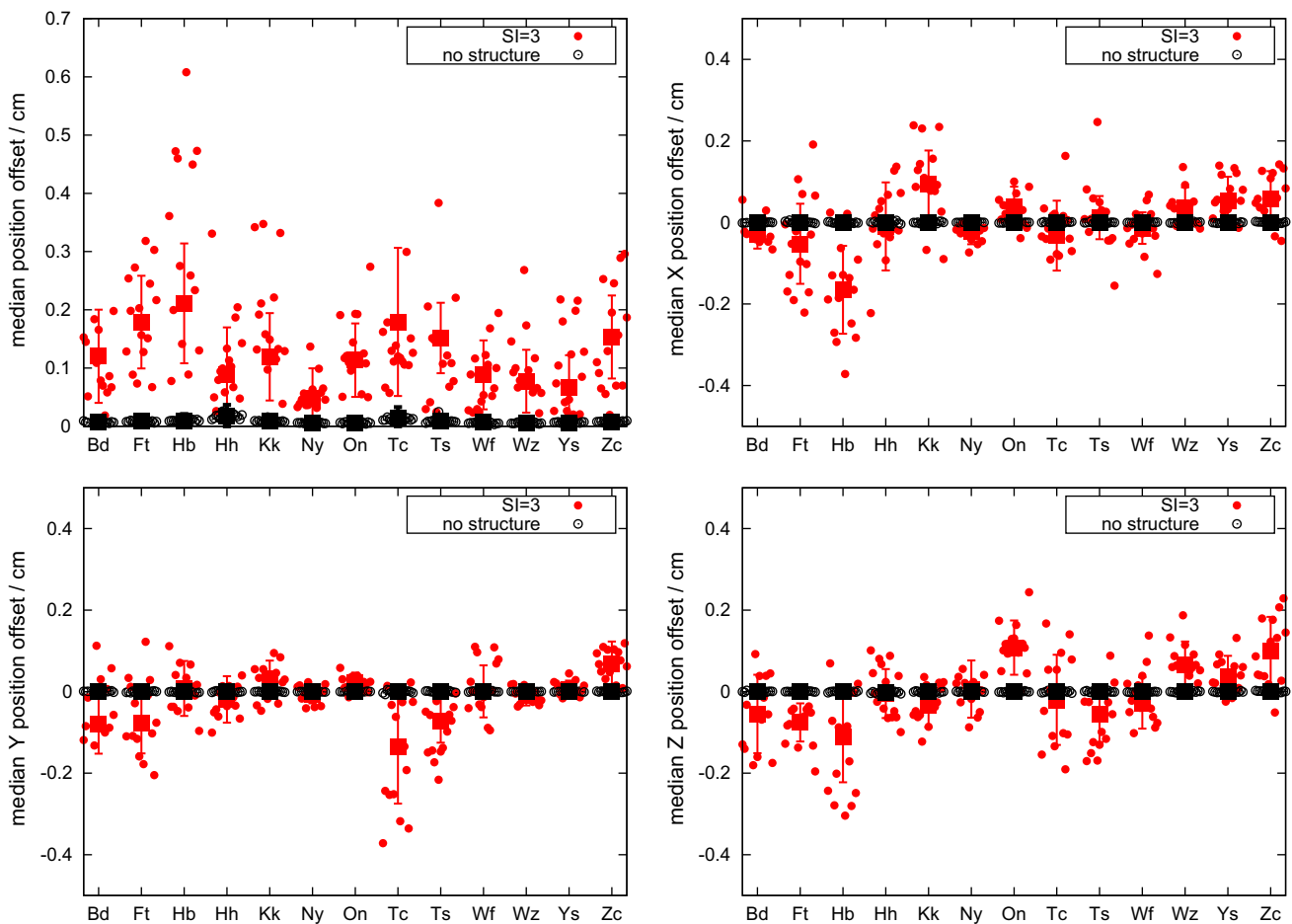


Fig. 6 Median position offsets from catalogued values in structure-only SI = 3 simulations: total (*top left*), X (*top right*), Y (*bottom left*) and Z (*bottom right*). Every station (refer to Fig. 10 for station codes) has 15 points, one for each day of CONT11. Each of these points comprises 30 realisations (i.e. the same schedule simulated 30 times). In all cases, the position rms over this set of 30 realisations is <0.3 mm,

i.e. negligible compared to the median offset. *Filled symbols* indicate medians over 15 observing days for each station. *Error bars* are formal uncertainties associated with the median values. On average, simulations with a structure index of 3 mis-estimate station coordinates by 0.5–2.1 mm, depending on station

For station positions, the metrics we use are:

1. Difference between calculated and true station position, $\Delta\text{pos} = (\Delta x^2 + \Delta y^2 + \Delta z^2)^{1/2}$. This value is calculated for each realisation of each 24-h observing session. It is the most direct measure of the impact of source structure, but is only available to us in simulations because we know the “true” answer and therefore can calculate Δpos .
2. Rms in Δpos , $\sigma(\Delta\text{pos}) = \sigma \left[\left((\Delta x - \bar{\Delta x})^2 + (\Delta y - \bar{\Delta y})^2 + (\Delta z - \bar{\Delta z})^2 \right)^{1/2} \right]$. Here, $\bar{\Delta x}$, $\bar{\Delta y}$, $\bar{\Delta z}$ denote mean coordinate offsets over all realisations. This quantity is directly observable, and is a one-dimensional measure of station position repeatability.
3. Formal uncertainty associated with each station position estimate. Greater uncertainties are expected when group delays in multiple scans are inconsistent with each other; this is one effect of source structure.

We also use similar metrics to assess ERP solutions.

4.1.1 Station positions

We begin by comparing the accuracy of estimated station positions between solutions.

Figure 6 shows the median station position offsets from the catalogued values calculated for each station for each day of CONT11. Each point corresponds to a median over 30 realisations. Source structure index is kept constant (either none or structure index = 3) over each set of 30 realisations, but the 1-ps noise varies randomly. It is clear that derived station positions can vary significantly on a daily basis, by up to 6 mm from the true value. On the other hand, the variability due to terms other than source structure is very small: the position rms for each set of 30 realisations, for a given station on a given day is <0.3 mm. The reason this value is so small is because for each set of 30 realisations, the same source

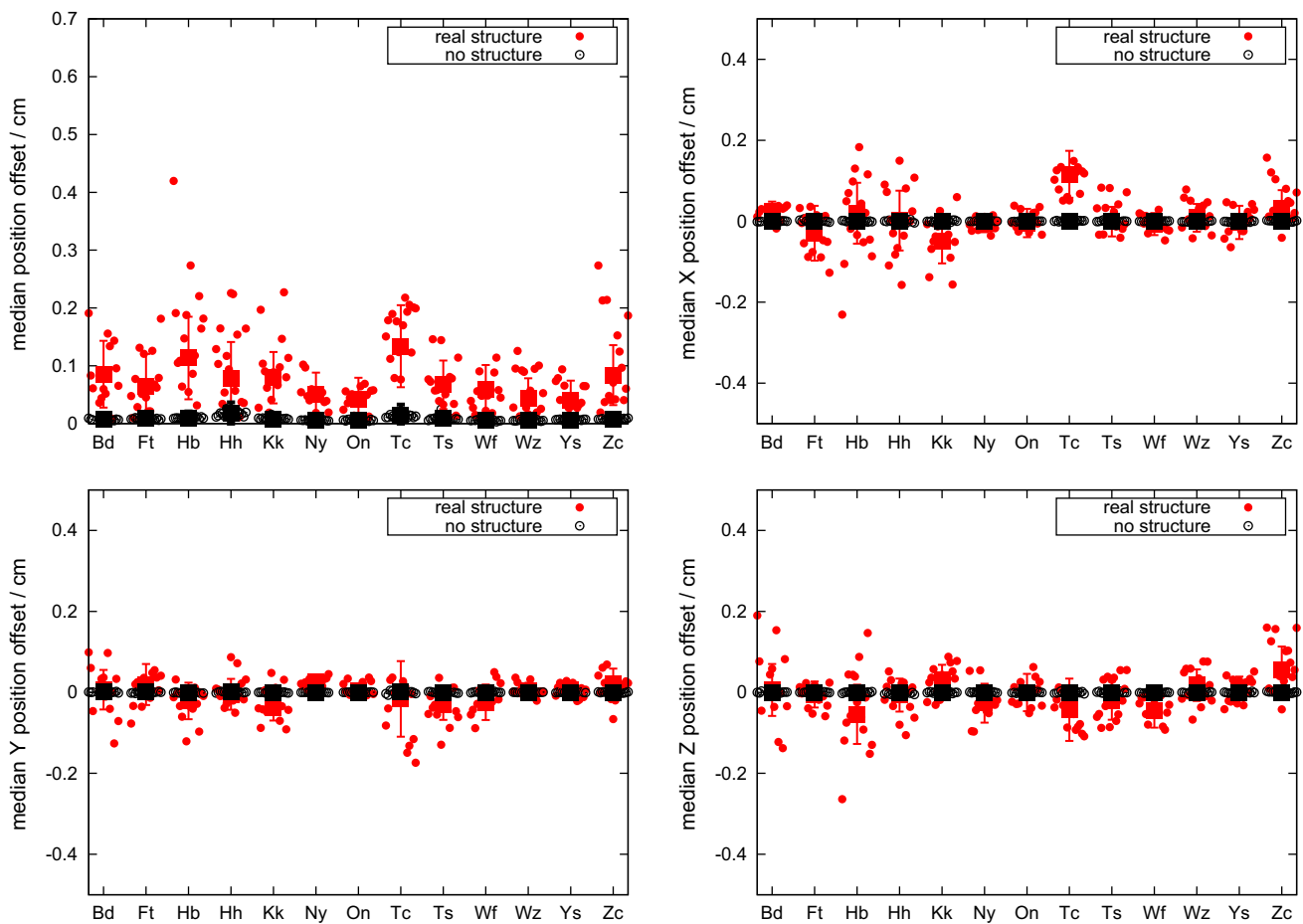


Fig. 7 Same as Fig. 6 but for real sources. On average, station positions are mis-estimated by 0.2–1.3 mm, depending on station, which is less than for SI = 3 simulations

structure is assumed. The median position offset (over all realisations) is different for all stations, ranging between 0.5 and 2.1 mm. Figure 6 shows that sources with structure index 3 can regularly affect station positions at the 1–2 mm level and occasionally on larger scales.

Sources with structure index of 3 are typically assumed to be on the cusp of being acceptable for IVS observations [e.g. Ma et al. (2009)]. In Fig. 7, we show a similar plot for real sources observed during CONT11. Although the effect is not as strong as for the SI = 3 catalogue, we find that station positions are still frequently affected the 1 mm level.

We can stack all simulations (30 realisations × 15 days) and repeat the above analysis. In Fig. 8 we do this, and compare the effects of different source structure on metrics 1→3 discussed above. This allows us to quantify the effects of different source structure as the schedules are changed.

As expected, simulations with higher source structure give larger formal uncertainties (due to worse residuals), and also higher median offset values (i.e. less accurate solutions). In general, they also yield larger scatter in calculated positions ($\sigma(\Delta\text{pos})$, the “observable” quantity). In Fig. 9, we plot the

median values (over all stations) of each position metric. Clearly the scatter in all values increases as source structure is increased. At this point, we can compare our simulated catalogues with results using the “real” source structure catalogue. Figure 9 shows that station position errors due to real source structure are somewhere between the SI = 2 and SI = 3 values (closer to SI = 2 for the median offset and rms metrics, and between SI = 2 and SI = 3 for the median uncertainty), consistent with the distribution of observed structure indices in Fig. 5. The three position metrics for real sources are in the range 0.25–0.6 mm. Our simulation results are in good agreement with simple analytical estimates: structure indices of 1, 2, 3, 4 should correspond to median group delay errors of 0.3, 1.0, 3 and 10 mm on a median Earth-bound baseline, respectively, and hence half these numbers for each station.

We note that the median offsets in station position are consistently higher than either the rms or formal uncertainties, regardless of the amount of source structure. Figures 6 and 7 explain this result: most of the time, the estimated coordinates of each station are shifted in a similar direction for each

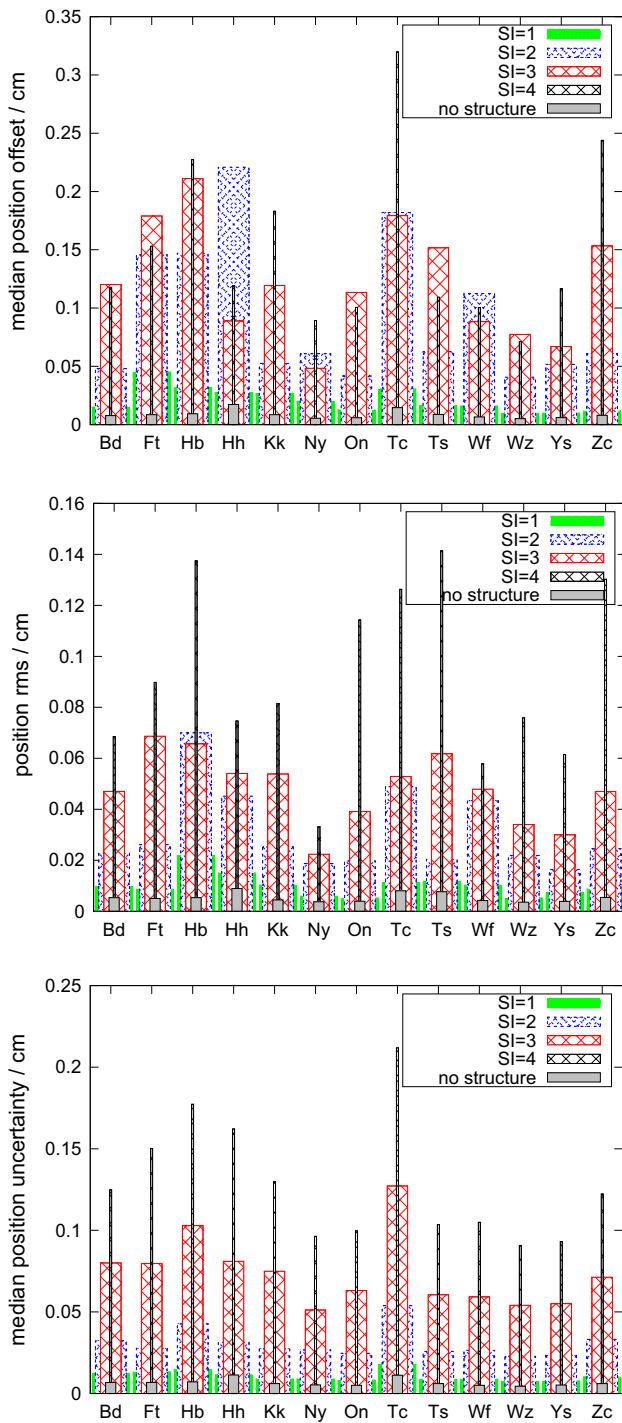


Fig. 8 Stacked position offsets in structure-only simulations. Simulations with large source structure indices have higher median position offsets (*top panel*), larger $\sigma(\Delta\text{pos})$ values (*middle panel*), and larger formal uncertainties (*bottom panel*). Note that the $\sigma(\Delta\text{pos})$ values have been de-biased, and represent scatter about mean positions; these mean positions will in general be different from the true positions (see Fig. 6). For this reason, $\sigma(\Delta\text{pos})$ values (*middle panel*) are typically smaller than median offsets (*top panel*), as seen in Fig. 9

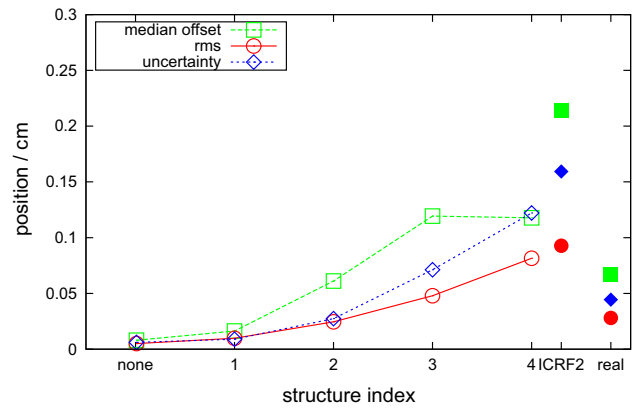


Fig. 9 Effects of source structure on station coordinate offsets (measured–true value, shown in *green*), debiased rms (*red*) and median formal uncertainty (*blue*) over 15 days of CONT11, in structure-only simulations. Median values over all stations are shown. *Filled symbols* are for the mock ICRF2 and real observed distribution of source structure

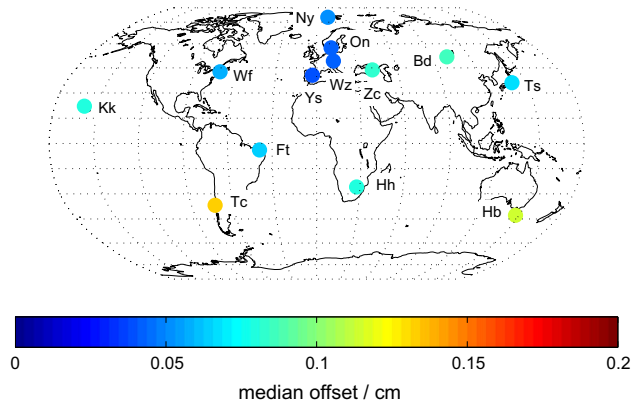


Fig. 10 Median station position offsets for the observed distribution of structure in a structure-only simulation. The most isolated stations have the largest position offsets from “true” values

day of the CONT11 campaign. This is most likely due to the quasars being observed in a similar way (i.e. with the same baselines at similar times) from one session to the next, presumably as an artefact of the scheduling process. This can yield repeatable, inaccurate solutions for which the offset from the true station position can be quite large despite the low rms and formal uncertainty.

4.1.2 Network effects

Some stations show noticeably worse station position repeatability for all values of the structure index. Figure 10 shows that these appear to be some of the most isolated stations [TIGO (Tc) and Hobart (Hb)]. While in real obser-

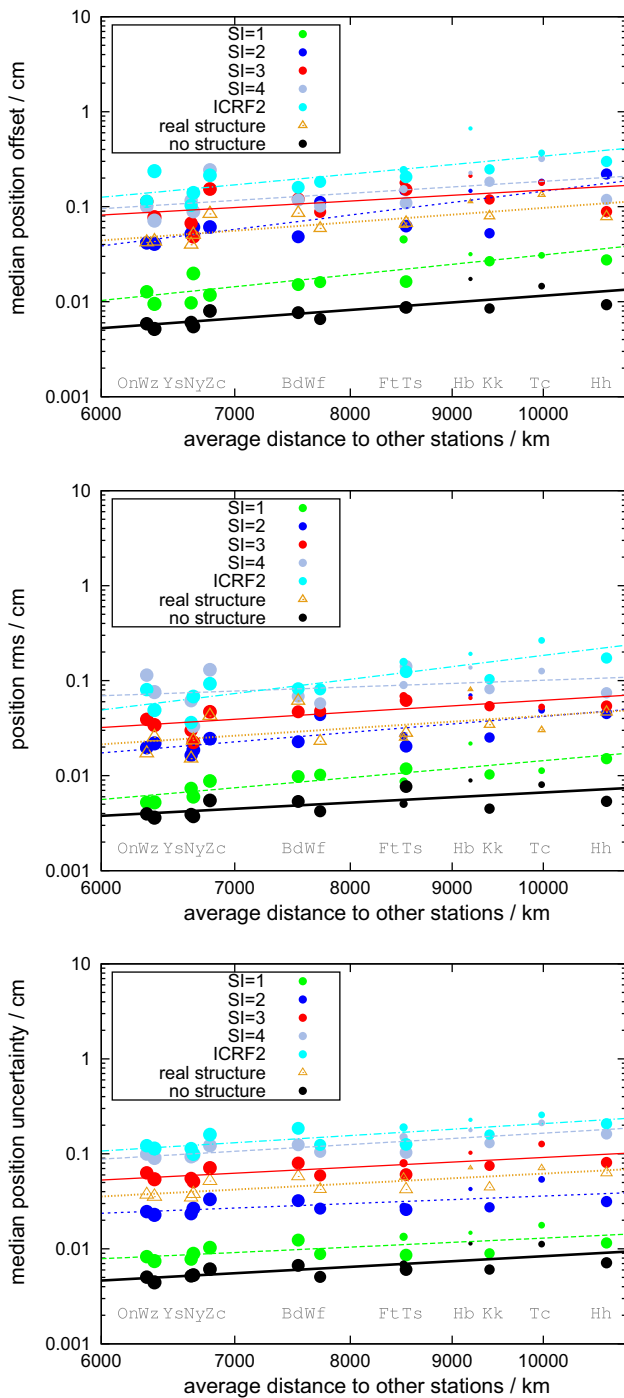


Fig. 11 Station position accuracy in structure-only simulations depends on network geometry. Abscissa is the average distance between the station of interest and all other stations in the CONT11 campaign. *Top* median offset from catalogue position; *middle* position rms; *bottom* median formal uncertainty. Each point represents one of 13 stations involved in CONT11. Symbol size is proportional to the logarithm of the average number of observations made by that station in a 24-h session. Lines are unweighted linear fits, included as a useful visual guide

variations factors such as dish size (e.g. 6 m at TIGO compared with 32 m at Badary and Zelenchukskaya, a factor of 30 difference in collecting area) are important, we do not simulate

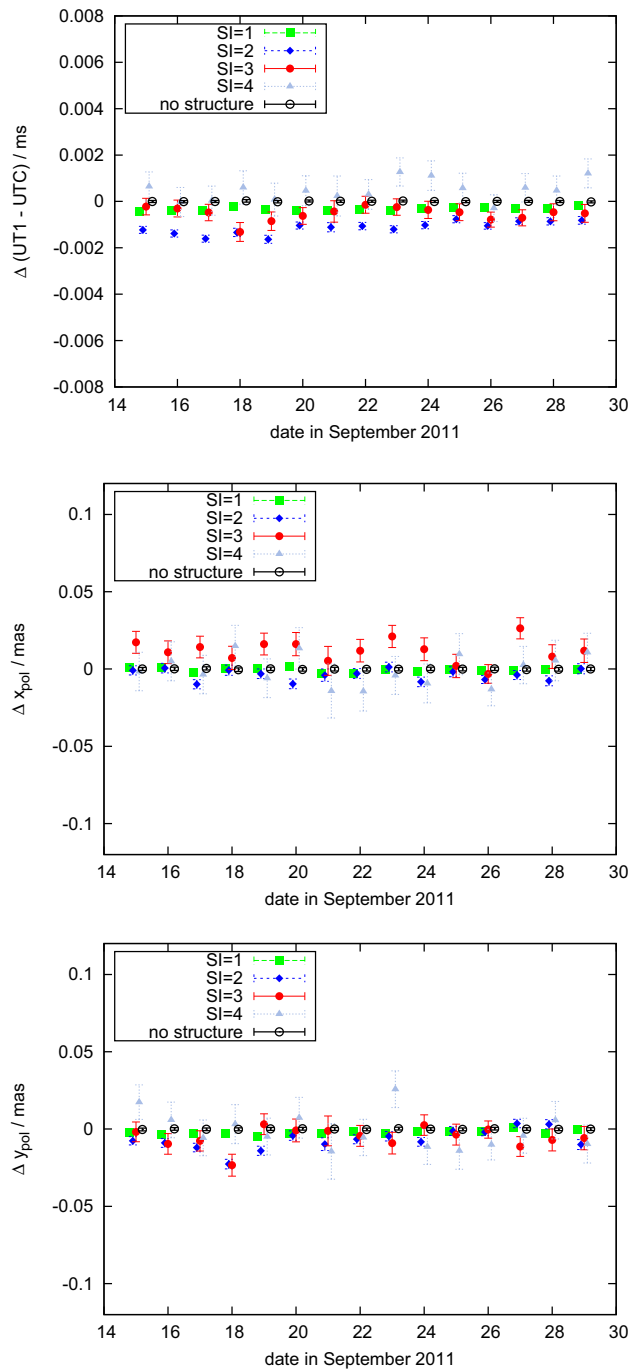


Fig. 12 Accuracy of (UT1-UTC) (*top*), x_{pol} (*middle*) and y_{pol} (*bottom*) measurements for each day in structure-only simulations. Points are median offsets over 30 realisations of each CONT11 session, and error bars are median formal uncertainties on the measurement. For all 15 days of CONT11, the rms (between 30 realisations) is negligible compared to these uncertainties. The true value of the ordinate is zero

this effect here, noting that schedules are optimised to yield similar sensitivity at all stations. The difference in dish size does, however, affect the total number of observations made by each station. We also expect network geometry to play an important role.

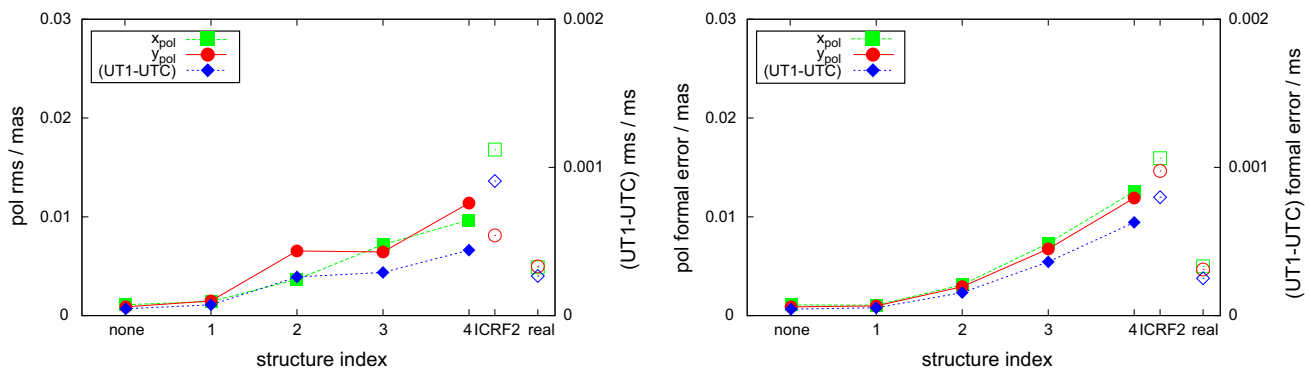


Fig. 13 Effects of source structure on rms of ERP offsets (measured–true value) over 15 days (*left panel*), and median formal uncertainty (*right panel*) for x_{pol} , y_{pol} and (UT1–UTC), in structure-only simula-

tions. *Open symbols* are for the mock ICRF2 distribution of structure indices, and real source structure

We crudely quantify network geometry by considering the average distance from the antenna of interest to all other stations participating in CONT11. Figure 11 plots the three station position quality metrics as a function of network geometry, for all our simulations. Stations located close to other antennas have much better determined positions. Importantly, at a fixed average distance, the source structure signal is very clear. Another way of quantifying the network effect is by considering the total number of observations made by each station; this is represented by symbol size in Fig. 11. Both station isolation and total number of observations are important to position accuracy. These two quantities are often (but not always) related: isolated stations typically make less observations in a given session, and hence have less accurate positions. Note that simulations of ICRF2 distribution of structure indices show position errors and scatter that are similar to the structure index 4 simulations, despite the median structure index of ICRF2 sources being 2.75. This is likely due to a relatively small number of sources with large structure indices (compare the ICRF2 histogram in the left panel of Fig. 4 with SI = 3 and 4 histograms in the right panel of Fig. 3). As discussed above, frequently observed sources typically have much less structure than sources drawn at random from ICRF2. As a result, real source structure for CONT11 sources contributes somewhat more than the SI = 2 and less than SI = 3 catalogues. We note that for real CONT11 sources, the median structure index weighted by number of observations toward each source is 2.7.

4.1.3 Earth rotation parameters

Finally, we consider the accuracy of ERP estimates. In particular, we focus on polar motion (x_{pol} and y_{pol} , describing the position of the celestial intermediate pole (CIP) in an Earth-fixed frame) and dUT1 (UT1–UTC) containing irreg-

ularities in the rotational speed around the CIP. In Fig. 12 we show the deviation from the true values and formal uncertainties of (UT1–UTC), x_{pol} and y_{pol} for each day. Since we did not simulate any Earth rotation variations, the expected (true) values are zero. Simulations with source structure yield much higher scatter and formal uncertainties (due to worse residuals) than simulations for point-like quasars. Because for a given schedule the observed source structure is identical for all 30 realisations, the rms values (within these realisations) are negligible compared to the medians: $\sigma_{x_{\text{pol}}}, \sigma_{y_{\text{pol}}} \leq 0.001$ mas and $\sigma_{\text{dUT1}} \leq 5 \times 10^{-5}$ ms.

We can quantify the contribution of source structure to errors in ERP determination by comparing both rms in ERP errors, and formal uncertainties, for each suite of simulations. This is shown in Fig. 13. Clearly there is a strong dependence of ERP accuracy on the source structure index, as expected. For real sources, rms and formal uncertainties for the polar motion components are ~ 5 μas , which is around 10 % of the present day accuracies for these parameters achieved with VLBI (50–80 μas , Schuh and Behrend 2012); a similar result is found for UT1–UTC. As we discuss below, these findings are consistent with the 0.25–0.6 mm error in station positions (Fig. 9) induced by source structure.

While both the rms and formal uncertainties in ERP estimates increase with structure, Fig. 12 shows that in some cases there may be a non-zero systematic offset in ERPs even for relatively small (SI = 2) structure indices. This offset in ERPs is related to a similar systematic offset in station positions (Figs. 6 and 7, where for each coordinate the offset in station position is in the same direction in most CONT11 sessions), and hints at the complex interplay between source structure and scheduling which affects all derived parameters. A detailed investigation of these effects is deferred to a future paper.

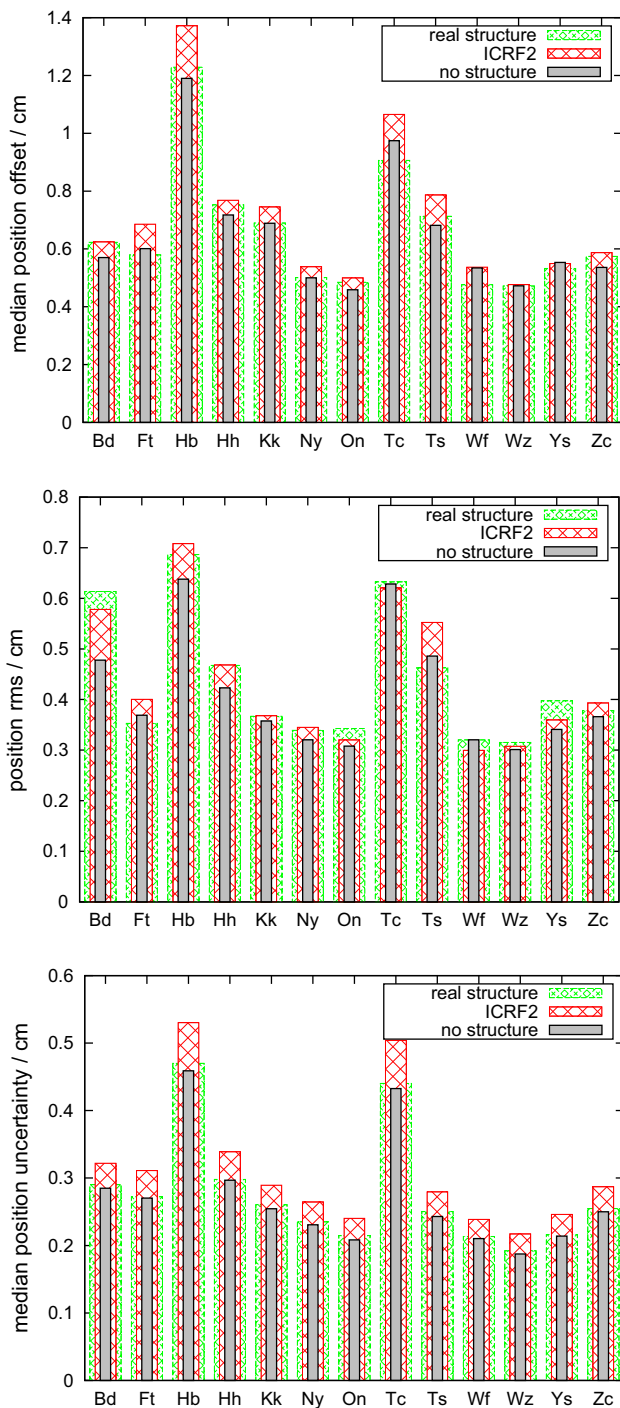


Fig. 14 Stacked position offsets for the full simulations. The signature is much less clear than in structure-only simulations (Fig. 8), with troposphere and clocks dominating the median position offsets (*top panel*), $\sigma(\Delta\text{pos})$ values (*middle panel*), and formal uncertainties (*bottom panel*)

4.2 Full simulations

The above simulations establish the importance of source structure to geodetic VLBI measurements. Extensive simulation work (e.g. Pany et al. 2011) has previously identified

tropospheric turbulence as a key limitation in such measurements. For our “full” simulations, we therefore model source structure as above, with 1 ps of white noise, and also simulate and solve for clocks and the wet troposphere in the standard way. The simulations were run with the following parameters: $C_n = 1.66 \times 10^{-7} \text{ m}^{-1/3}$, $H = 2000 \text{ m}$, $v_e = 5.66 \text{ m s}^{-1}$, $d_h = 200 \text{ m}$, $wzd_0 = 250 \text{ mm}$, $v_n = 5.66 \text{ m s}^{-1}$, $dh_{\text{seg}} = 2 \text{ h}$. Here, C_n is the refractive index structure constant and H is the effective height until which C_n is assumed to be constant; above H , there is no turbulence. These two parameters are the most important for the “strength” of the troposphere. d_h is the height increment for the vertical integration, dh_{seg} is the correlation time (i.e. the observations are correlated over this time period); wzd_0 is the initial zenith wet delay; and v_n and v_e are the wind speed in the north and east directions, respectively. More details on these parameters can be found in Pany et al. (2011). The clock stability was 1×10^{-14} at 50 min. These values are typical for geodetic VLBI observations (e.g. Nilsson et al. 2007), and consistent with CONT05 and CONT08 work of Nilsson and Haas (2010).

4.2.1 Station positions

As before, we stack all simulations (30 realisations \times 15 days); this is shown in Fig. 14. In Fig. 15, we show the effect of different levels of source structure on station coordinate estimates.

The source structure effect is relatively small, with the troposphere and clocks dominating. Comparison of Figs. 15 and 9 shows that for real sources, structure contributes about 10% of the station position error. Note also that the stochastic nature of the troposphere and clocks can affect solutions significantly: for station Yebes for example, inclusion of source structure yields slightly smaller values of median offset from the true value.

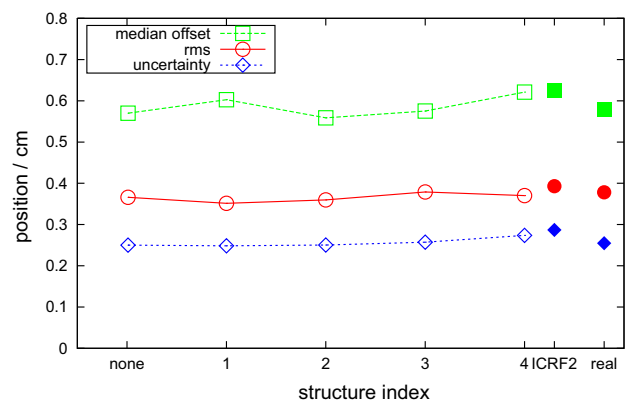


Fig. 15 Effects of source structure on station coordinates in full simulations. As in Fig. 9, median values over all stations are shown. Source structure effects are masked by the troposphere and clocks

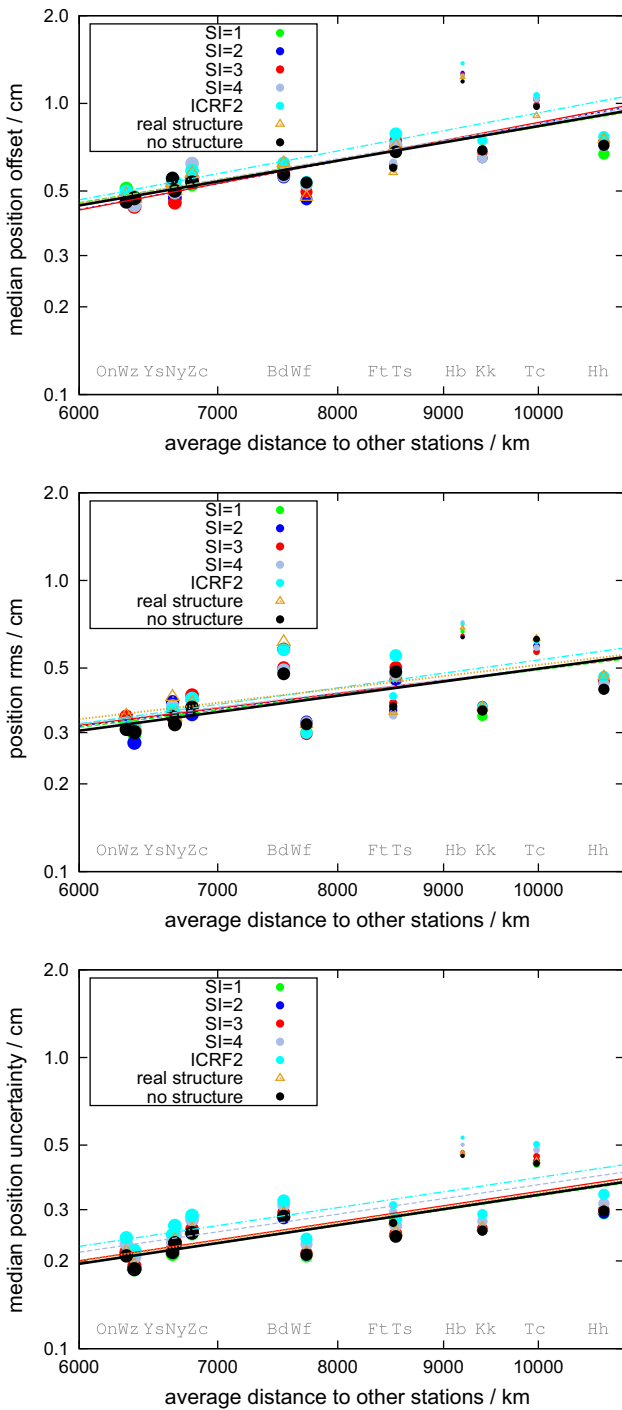


Fig. 16 As in Fig. 11 but for full simulations, including clocks and troposphere

Figures 15 and 16 show that source structure can still have a slight effect on station positions, even when tropospheric turbulence is included, if the sources are selected badly (e.g. if the “full” ICRF2, which includes a number of bad sources, is selected). A comparison of simulations without source structure and ICRF2 structure index distribution (Fig. 14) shows

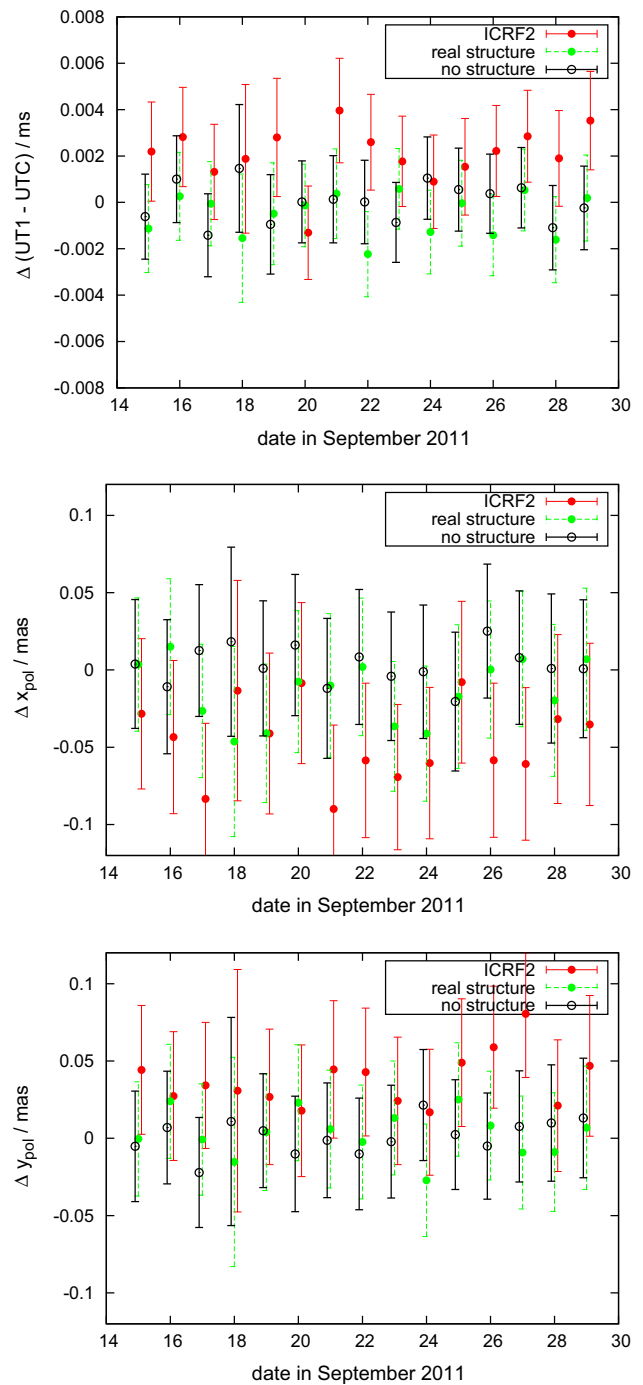


Fig. 17 Accuracy of (UT1-UTC) (top), x_{pol} (middle) and y_{pol} (bottom) measurements for each day of the full simulations. Points are medians over 30 realisations of each CONT11 session, and error bars are median formal uncertainties on the measurement. The true value of the ordinate is zero

that inclusion of source structure can affect the median offsets and uncertainties in station positions by up to 10–15%. Choosing sources to predominantly have structure indices below 3 (as is the case with the real CONT11 sources) reduces this contribution to below the 10% level.

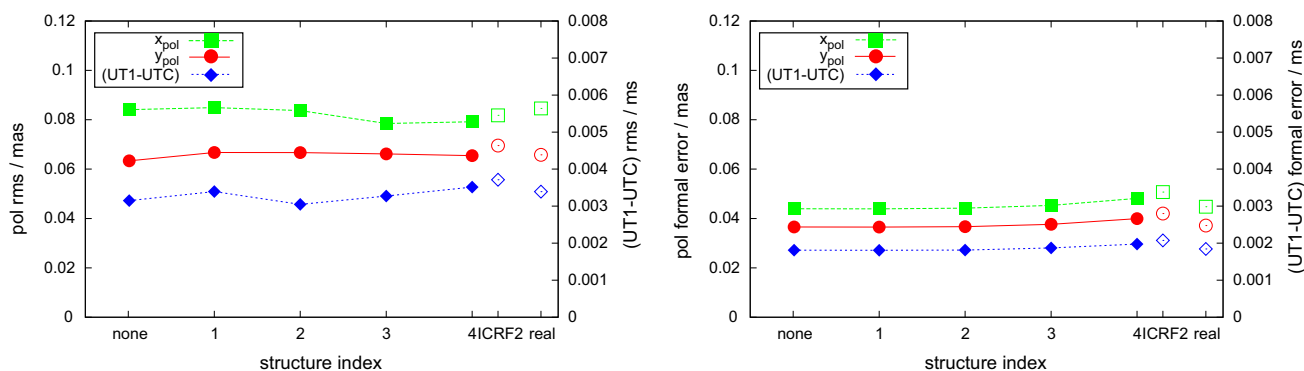


Fig. 18 Effects of source structure on rms of ERP offsets (measured–true value) (*left panel*) and median formal uncertainty (*right panel*) for x_{pol} , y_{pol} and (UT1-UTC). These results are for full simulations

4.2.2 Earth orientation parameters

In Fig. 17 we consider the effects of source structure on ERPs in our “full” simulations.

As for structure-only simulations, we can compare ERP estimates for different source structure catalogues (Fig. 18). Simulations with large amounts of source structure (SI = 3 or more) show slightly larger uncertainty in ERPs than those without source structure; however this effect is not seen for real sources. No source structure signature is at all apparent in the rms of ERP offsets, due to the extra “noise” added by troposphere and clocks. Comparison of Figs. 12 and 17 suggests that for real CONT11 sources, structure contributes to the ERPs at approximately the 10 % level also found for station positions.

5 Conclusions and future work

We performed simulations of quasar structure in geodetic VLBI observations. Using the CONT11 observing campaign as a test bed, we found that source structure can induce regular station position measurement errors of up to a few mm if badly selected sources (i.e. with large amounts of structure) are used. For real sources observed during CONT11, the median errors in station position are of order 0.2–0.6 mm. These effects are about 10 % of the ~ 5 mm errors induced by tropospheric effects. Our simulations confirm analytical estimates that source structure is an important consideration if VLBI station position accuracy is to be realised at the millimetre level; and that sources with structure indices ≤ 2 should be used for accurate astrometric and geodetic work, as previously suggested by Fey and Charlot (1997), Fey and Charlot (2000).

The source structure simulator offers a number of further possibilities for investigating the effects of source structure, and development of mitigation strategies. Previous attempts (e.g. Petrov 2007) to correct for source structure by using

VLBI images of radio sources, have not resulted in an obvious improvement of solutions (as measured by station position rms). At least in part, this could be due to radio source structure evolving on timescales of months and years (Lister et al. 2009; Shabala et al. 2014); understanding the effects of this evolution on geodetic VLBI measurements is therefore important. Furthermore, because observed quasar structure changes with observing baseline, repeated measurements of astrometric positions of radio sources encode important information about source structure. Compact sources are more astrometrically stable (Ojha et al. 2004; Ma et al. 2009; Moór et al. 2011; Schaap et al. 2013), as are radio sources that exhibit small time lags in flux density time series as a function of frequency (Shabala et al. 2014). Simulations offer a powerful new way of investigating these connections between radio source astrophysics, astrometry and geodesy.

Finally, source-based scheduling provides an immediate way of improving the reference frame accuracy. Although source structure varies on human timescales in most quasars, the jet direction remains similar in most objects. This astrophysical information can be used to optimise observing schedules through minimising the projected source structure for a given time–baseline pair, by observing only those sources for which the jet and baseline vectors are close to orthogonal. We intend to investigate this possibility by combining the VieVS scheduling tool (Sun et al. 2014) with the source structure simulator presented here.

Acknowledgments We thank the anonymous referees for their useful and constructive comments. S. S., J. M. and L. P. thank the Australian Research Council for Research Fellowships. We are grateful to Jim Lovell, Simon Ellingsen, John Dickey and Rob Schaap for useful discussions.

References

Böhm J, Böhm S, Nilsson T, Pany A, Plank L, Spicakova H, Teke K, Schuh H (2012) The New Vienna VLBI Software. In: Kenyon S, Pacino MC, Marti URS (eds) Proceedings of the 2009 IAG Sympo-

- sium, Buenos Aires, Argentina. Series: International Association of Geodesy Symposia, vol 136. 31 Aug–4 Sep 2009, pp 1007–1012 (ISBN 978-3-642-20337-4)
- Charlot P (1990) Radio-source structure in astrometric and geodetic very long baseline interferometry. *Astron J* 99:1309
- Fey AL, Charlot P (1997) VLBA observations of radio reference frame sources. II. Astrometric suitability based on observed structure. *Astrophys J Suppl Ser* 111:95
- Fey AL, Charlot P (2000) VLBA observations of radio reference frame sources. III. Astrometric suitability of an additional 225 sources. *Astrophys J Suppl Ser* 128:17
- Lister ML, Cohen MH, Homan DC, Kadler M, Kellermann KI, Kovalev YY, Ros E, Savolainen T, Zensus A (2009) MOJAVE: monitoring of jets in active galactic nuclei with VLBA experiments. VI. Kinematics analysis of a complete sample of blazar jets. *Astron J* 137:3718
- Ma C et al (2009) IERS technical note. No. 35. <http://www.iers.org/IERS/EN/Publications/TechnicalNotes/tn35.html>. Accessed 1 May 2015
- Moór A, Frey S, Lambert SB, Titov OA, Bakos J (2011) On the connection of the apparent proper motion and the VLBI structure of compact radio sources. *Astron J* 141:178
- Nilsson T, Haas R, Elgered G (2007) Simulations of atmospheric path delays using turbulence models. In: Böhm J, Pany A, Schuh H (eds) Proceedings of the 18th European VLBI for Geodesy and Astrometry Working Meeting, 1213 April 2007, Geowissenschaftliche Mitteilungen, Heft Nr. 79, Schriftenreihe der Studienrichtung Vermessung und Geoinformation, Technische Universität Wien, pp 175–180 (ISSN 18118380)
- Nilsson T, Haas R (2010) Impact of atmospheric turbulence on geodetic very long baseline interferometry. *J Geophys Res* 115:B03407. doi:10.1029/2009JB006579
- Ojha R, Fey AL, Jauncey DL, Lovell JEJ, Johnston KJ (2004) Milliarcsecond structure of microarcsecond sources: comparison of scintillating and non-scintillating extragalactic radio sources. *Astrophys J* 614:607
- Pany A, Böhm J, MacMillan D, Schuh H, Nilsson T, Wresnik J (2011) Monte Carlo simulations of the impact of troposphere, clock and measurement errors on the repeatability of VLBI positions. *J Geodesy* 85(1):39–50. doi:10.1007/s00190-010-0415-1
- Petrachenko B, Niell A, Behrend D, Corey B, Böhm J, Charlot P, Collioud A, Gipson J, Haas R, Hobiger T, Koyama Y, MacMillan D, Malkin Z, Nilsson T, Pany A, Tuccari G, Whitney A, Wresnik J (2009) Design aspects of the VLBI2010 system: progress report of the IVS VLBI2010 Committee, NASA/TM-2009-214180
- Petrov L (2007) Proceedings of the 18th European, VLBI for geodesy and astrometry working meeting. In: Böhm J, Pany A, Schuh H (eds) pp 141–146
- Plag H-P, Pearlman M (eds) (2009) Global geodetic observing system-meeting the requirements of a global society on a changing planet in 2020. Springer Verlag, Berlin
- Schaap RG, Shabala SS, Ellingsen SP, Titov OA, Lovell JEJ (2013) Scintillation is an indicator of astrometric stability. *Monthly Notices Roy Astron Soc* 434:585
- Schuh H, Behrend D (2012) VLBI: a fascinating technique for geodesy and astrometry. *J Geodyn* 61:68
- Shabala SS, Rogers JG, McCallum JN, Titov O, Blanchard J, Lovell JEJ, Watson CS (2014) The effects of frequency-dependent quasar evolution on the celestial reference frame. *J Geodesy* 88:575
- Sun J, Böhm J, Nilsson T, Krásná H, Böhm S, Schuh H (2014) New VLBI2010 scheduling strategies and implications on the terrestrial reference frames. *J Geodesy* 88:449